182485: migmatitic gneiss, Burkin prospect

(Madura Province)

Location and sampling

LOONGANA (SH 52-9), SLEEPER CAMP (4137)
MGA Zone 52, 230702E 6637028N

Sampled on 17 August 2010

This sample was collected from diamond drillcore from hole BKD2, located on the Burkin prospect, at a depth of 271.38 – 272.08 m. The hole was drilled in 2009 by Gunson Resources Ltd, and was co-funded through the Exploration Incentive Scheme. The drillhole is located on the Nullarbor Plain, approximately 14.5 km east-northeast of Double Pump Bore, 7.4 km northeast of Middle Bore, and 6.1 km west of Sleeper Camp.

Tectonic unit/relations

The sample is from drillhole BKD2, which penetrated Precambrian basement rocks of the Madura Province, beneath the Mesozoic–Cenozoic Eucla Basin, at a depth of 248.7 m; the total depth of the hole was 400 m. The Madura Province is an area of basement bounded by the Rodona Shear Zone in the west, and the Mundrabilla Shear Zone in the east (Spaggiari et al., 2012). BKD2 was drilled to investigate coincident magnetic and gravity anomalies, potentially related to Proterozoic nickel-sulfide mineralization (Benton, 2009). The Precambrian rocks in BKD2 comprise metagabbro, garnet-bearing migmatitic granitic gneiss (of which the present sample is representative), and meta-ultramafic rocks (Benton, 2009). Deformed neosomes in the migmatitic gneiss crosscut an earlier phase of folding, indicating that these rocks have undergone at least two phases of deformation.

Previous geochronology from the Madura Province is sparse. Intrusive rocks from drillhole LNGD0002 on the Loongana prospect yielded an igneous crystallization age of 1415 ± 7 Ma (GSWA 178070, Nelson et al., 2005a), whereas microtonalite from a nearby drillhole (LNGD0001) yielded an igneous crystallization age of 1408 ± 7 Ma (GSWA 178071, Nelson et al., 2005b), and tonalite gneiss from the same core yielded an igneous crystallization age of 1407 ± 7 Ma (GSWA 178072, Nelson et al., 2005c).

Petrographic description

The sample is a recrystallized, hydrothermally altered, crudely banded, medium- to coarse-grained, garnet-bearing granitic gneiss. Its visually estimated mineralogy comprises 60% feldspar, 30% quartz, 4% epidote, 3% muscovite, 2% garnet, and accessory biotite, muscovite, iron-oxide minerals, zircon, and chlorite. Fine- to medium-grained feldspar and quartz grains are corroded and resorbed, and feldspars are heavily saussuritized. Garnet forms isolated corroded grains partly rimmed by epidote, muscovite, and chlorite. Iron-oxide minerals are altered to chlorite. The paragenetic sequence is: plagioclase, garnet, quartz, saussurite.

Zircon morphology

Zircons from this sample are subhedral, generally rounded, and colourless to black. The crystals are up to 300 µm long, and equant to elongate, with aspect ratios up to 5:1. In cathodoluminescence (CL) images, some crystals display faint indications of oscillatory zoning and homogeneous patches with little CL response. Some crystals contain apparently older cores. A CL image of representative zircons is shown in Figure 1.

Analytical details

This sample was analysed on 6–7 September 2011, using SHRIMP-B, and on 20 October 2011, using SHRIMP-B. Analyses 1.1 to 26.1 (spot numbers 1–26) were obtained during the first session, together with 14 analyses of the BR266 standard, which indicated an external spot-to-spot (reproducibility) uncertainty of 0.50% (1σ) and a $^{238}U/^{206}Pb^*$ calibration uncertainty of 0.12% (1σ). Analyses 2.2, 27.1, and 28.1 (spot numbers 27–29) were obtained during the second session, together with four analyses of the BR266 standard, which indicated an external spot-to-spot (reproducibility) uncertainty of 1.23% (1σ) and a $^{238}U/^{206}Pb^*$ calibration uncertainty of 0.62% (1σ). Calibration uncertainties are included in the errors of $^{238}U/^{206}Pb^*$ ratios and dates listed in Table 1. Common-Pb corrections were applied to all analyses using contemporaneous isotopic compositions determined according to the model of Stacey and Kramers (1975).

Results

Twenty-nine analyses were obtained from 28 zircons. Results are listed in Table 1, and are shown in a concordia diagram (Fig. 2).

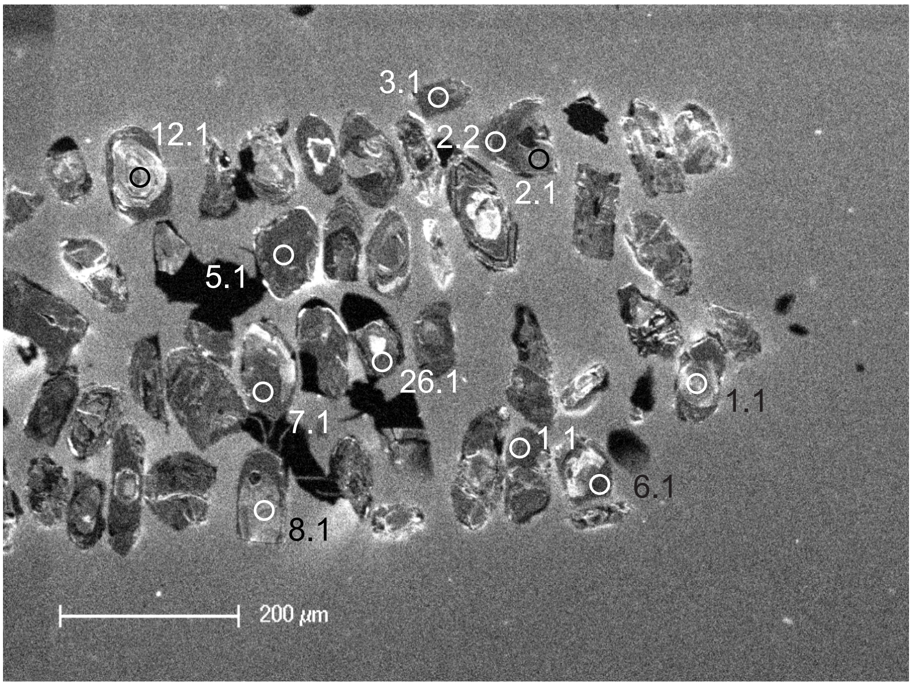

Figure 1. **Cathodoluminescence image of representative zircons from sample 182485: migmatitic gneiss, Burkin prospect. Numbered circles indicate the approximate positions of analysis sites.**

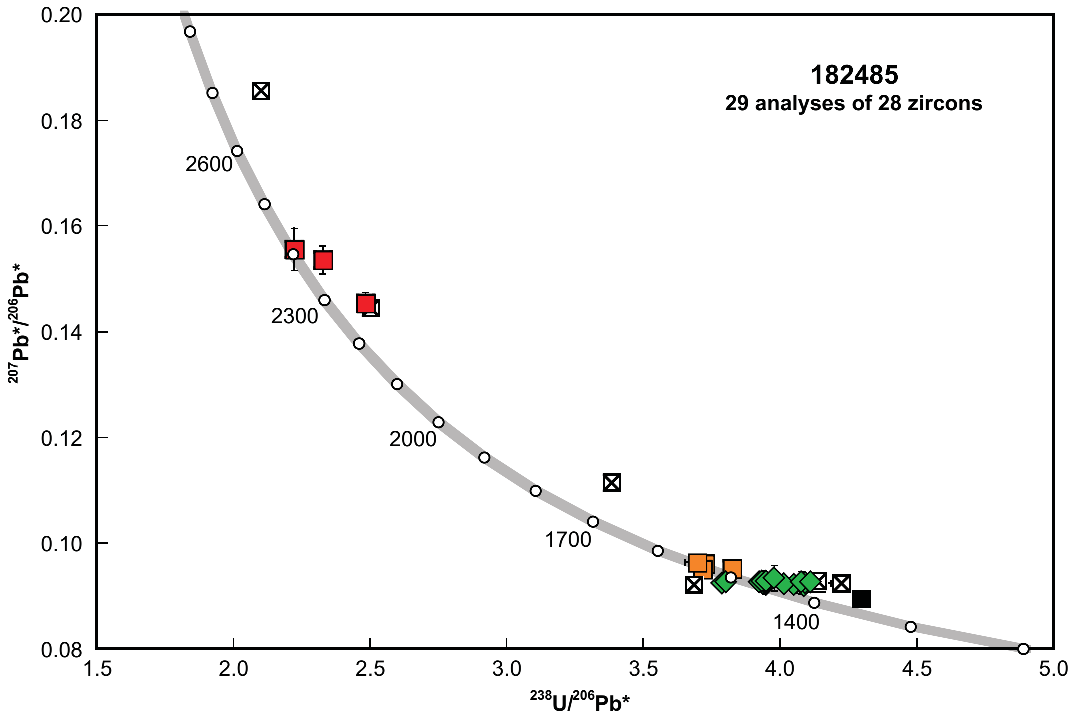

Figure 2. **U–Pb analytical data for zircons from sample 182485: migmatitic gneiss, Burkin prospect. Red squares indicate Group S (detrital zircons); black square indicates Group P (radiogenic-Pb loss); green diamonds indicate Group M (metamorphic zircon rims); orange squares indicate Group Z (possible radiogenic-Pb loss); crossed squares indicate Group D (discordance >5%).**

Table 1. Ion microprobe analytical results for zircons from sample 182485: migmatitic gneiss, Burkin prospect

Group ID	Spot no.	Grain. spot	^{238}U (ppm)	^{232}Th (ppm)	$^{232}Th/^{238}U$	f204 (%)	$^{238}U/^{206}Pb$	± 1σ	$^{207}Pb/^{206}Pb$	± 1σ	$^{238}U/^{206}Pb^*$	± 1σ	$^{207}Pb^*/^{206}Pb^*$	± 1σ	$^{238}U/^{206}Pb^*$ date (Ma)	±1σ	$^{207}Pb^*/^{206}Pb^*$ date (Ma)	±1σ	Disc. (%)
S	2	2.1	1123	369	0.34	-0.002	2.483	0.017	0.14544	0.00192	2.483	0.017	0.14546	0.00192	2182	13	2293	23	4.9
S	13	13.1	638	313	0.51	0.015	2.325	0.017	0.15375	0.00259	2.326	0.017	0.15362	0.00259	2306	14	2387	29	3.4
S	18	18.1	717	180	0.26	0.021	2.222	0.016	0.15578	0.00396	2.222	0.016	0.15559	0.00396	2395	14	2408	43	0.5
P	26	26.1	665	24	0.04	0.209	4.288	0.030	0.09146	0.00035	4.297	0.030	0.08967	0.00046	1349	9	1418	10	4.9
M	21	21.1	411	203	0.51	0.054	4.087	0.033	0.09236	0.00047	4.089	0.033	0.09190	0.00051	1410	10	1465	11	3.8
M	19	19.1	896	687	0.79	0.075	3.948	0.027	0.09274	0.00031	3.950	0.027	0.09210	0.00034	1455	9	1469	7	1.0
M	3	3.1	705	73	0.11	0.132	4.048	0.030	0.09328	0.00156	4.053	0.031	0.09215	0.00158	1422	10	1470	33	3.3
M	16	16.1	599	139	0.24	0.194	4.008	0.030	0.09394	0.00041	4.015	0.030	0.09228	0.00051	1434	10	1473	11	2.7
M	11	11.1	3659	320	0.09	0.041	3.789	0.022	0.09277	0.00016	3.790	0.022	0.09242	0.00017	1509	8	1476	4	-2.3
M	10	10.1	497	19	0.04	0.135	4.087	0.093	0.09365	0.00042	4.093	0.093	0.09249	0.00049	1409	29	1477	10	4.6
M	15	15.1	2090	302	0.15	0.008	3.802	0.023	0.09266	0.00020	3.803	0.023	0.09259	0.00020	1505	8	1479	4	-1.7
M	17	17.1	732	91	0.13	0.154	4.074	0.029	0.09389	0.00200	4.080	0.029	0.09256	0.00202	1413	9	1479	41	4.5
M	9	9.1	856	147	0.18	0.021	3.940	0.026	0.09278	0.00030	3.941	0.026	0.09260	0.00031	1458	9	1480	6	1.5
M	6	6.1	1203	93	0.08	0.030	3.924	0.025	0.09295	0.00024	3.925	0.025	0.09269	0.00025	1463	8	1482	5	1.2
M	12	12.1	188	191	1.05	0.120	3.930	0.040	0.09381	0.00072	3.935	0.040	0.09278	0.00083	1460	13	1483	17	1.6
M	23	23.1	912	788	0.89	0.057	3.948	0.027	0.09330	0.00031	3.951	0.027	0.09281	0.00034	1455	9	1484	7	2.0
M	1	1.1	263	466	1.83	0.024	3.978	0.034	0.09357	0.00236	3.979	0.034	0.09336	0.00237	1445	11	1495	48	3.3
M	28	27.1	229	172	0.77	0.523	3.812	0.066	0.09801	0.00082	3.832	0.066	0.09352	0.00129	1495	23	1498	26	0.2
Z	5	5.1	1454	432	0.31	0.035	3.715	0.023	0.09544	0.00022	3.717	0.023	0.09514	0.00023	1536	9	1531	5	-0.3
Z	24	24.1	1049	274	0.27	0.088	3.821	0.025	0.09599	0.00028	3.824	0.025	0.09523	0.00031	1498	9	1533	6	2.3
Z	14	14.1	505	206	0.42	0.012	3.721	0.028	0.09620	0.00040	3.722	0.028	0.09609	0.00041	1534	10	1550	8	1.0
Z	29	28.1	1047	371	0.37	0.043	3.719	0.055	0.09664	0.00037	3.721	0.055	0.09627	0.00039	1534	20	1553	8	1.2
D	20	20.1	1789	153	0.09	0.012	3.683	0.023	0.09231	0.00019	3.684	0.023	0.09221	0.00020	1548	8	1472	4	-5.2
D	22	22.1	610	293	0.50	0.263	4.213	0.030	0.09473	0.00038	4.224	0.030	0.09247	0.00052	1370	9	1477	11	7.3
D	4	4.1	868	55	0.07	0.058	4.131	0.028	0.09303	0.00031	4.134	0.028	0.09253	0.00034	1397	8	1478	7	5.5
D	7	7.1	1002	126	0.13	0.177	4.130	0.027	0.09441	0.00029	4.138	0.027	0.09289	0.00037	1395	8	1486	7	6.1
D	25	25.1	1450	139	0.10	0.015	3.383	0.021	0.11165	0.00125	3.383	0.021	0.11152	0.00126	1669	9	1824	20	8.5
D	27	2.2	387	315	0.84	-0.039	2.528	0.040	0.14494	0.00064	2.527	0.040	0.14529	0.00065	2149	29	2291	8	6.2
D	8	8.1	179	102	0.59	0.057	2.099	0.022	0.18616	0.00078	2.100	0.022	0.18565	0.00080	2511	22	2704	7	7.2

Interpretation

The analyses are concordant to slightly discordant (Fig. 2). Seven analyses are >5% discordant. The dates obtained from these seven analyses (Group D; Table 1) are imprecise or unreliable, and are considered not geologically significant. The remaining 22 analyses define four groups, based on their $^{207}Pb^{*}/^{206}Pb^{*}$ ratios.

Group S comprises three analyses of three zircon cores (Table 1), which yield $^{207}Pb^{*}/^{206}Pb^{*}$ dates of 2408–2293 Ma.

Group P comprises one analysis of a zircon rim (Table 1), which yields a $^{207}Pb^{*}/^{206}Pb^{*}$ date of 1418 ± 10 Ma (1σ).

Group M comprises 14 analyses of 14 zircon rims or discrete homogeneous crystals (Table 1), which yield a weighted mean $^{207}Pb^{*}/^{206}Pb^{*}$ date of 1478 ± 4 Ma (MSWD = 0.45).

Group Z comprises four analyses of four zircon cores (Table 1), which yield a weighted mean $^{207}Pb^{*}/^{206}Pb^{*}$ date of 1538 ± 17 Ma (MSWD = 3.1).

The dates of 2408–2293 Ma for the three analyses in Group S are interpreted as the ages of zircon-crystallizing rocks in the detrital source region(s), or as the ages of detrital components within sediments that have been reworked into this rock. Alternatively, if the protolith was an igneous rock, these analyses reflect inherited components, or c. 2450 Ma magmatic zircons that underwent Proterozoic radiogenic-Pb loss. The date of 1418 ± 10 Ma (1σ) for the single analysis of a zircon rim in Group P is interpreted to reflect minor ancient radiogenic-Pb loss.

The date of 1478 ± 4 Ma for the 14 analyses in Group M is interpreted as the age of new zircon growth associated with migmatization and high-grade metamorphism. This process may have been coeval with recrystallization of susceptible zircon cores.

The date of 1538 ± 17 Ma for the four analyses in Group Z is interpreted to reflect partial loss of radiogenic Pb from zircon cores, as suggested by their faded zoning in CL images, and by their high dispersion around the mean date. Alternatively, if the protolith of this gneiss was a sedimentary rock, it is possible that the analyses in Group Z represent unmodified detrital zircons, in which case the date of 1538 ± 17 Ma for the four analyses in Group Z represents a maximum age for deposition of the sedimentary precursor.

References

Benton, J 2009, Diamond Drilling at E69/1972, 19 August 2009 – 16 September 2009, Holes BKD1 – BKD2, Gunson Resources Limited's Burkin Nickel Project, well completion report: Digirock Pty Ltd, Perth, Western Australia, 18p. (unpublished).

Nelson, DR 2005a, 178070: amphibolite, Haig Cave; Geochronology Record 596: Geological Survey of Western Australia, 4p.

Nelson, DR 2005b, 178071: recrystallized biotite microtonalite, Haig Cave; Geochronology Record 597: Geological Survey of Western Australia, 4p.

Nelson, DR 2005c, 178072: tonalitic gneiss, Haig Cave; Geochronology Record 598: Geological Survey of Western Australia, 4p.

Spaggiari, CV, Kirkland, CL, Smithies, RH and Wingate, MTD 2012, What lies beneath — interpreting the Eucla basement, *in* GSWA 2012 extended abstracts: promoting the prospectivity of Western Australia: Geological Survey of Western Australia, Record 2012/2, p. 25–27.

Stacey, JS and Kramers, JD 1975, Approximation of terrestrial lead isotope evolution by a two-stage model: Earth and Planetary Science Letters, v. 26, p. 207–221.

Recommended reference for this publication

Kirkland, CL, Wingate, MTD and Spaggiari, CV 2012, 182485: migmatitic gneiss, Burkin prospect; Geochronology Record 1054: Geological Survey of Western Australia, 4p.

Data obtained: 20 October 2011

Data released: 30 June 2012